



Article

On the Use of Mechano-Chemically Modified Ground Tire Rubber (GTR) as Recycled and Sustainable Filler in Styrene-Butadiene Rubber (SBR) Composites

Javier Araujo-Morera , Reyes Verdugo-Manzanares, Sergio González, Raquel Verdejo , Miguel Angel Lopez-Manchado and Marianella Hernández Santana *

Institute of Polymer Science and Technology (ICTP-CSIC), Juan de la Cierva 3, 28006 Madrid, Spain; jaraujo@ictp.csic.es (J.A.-M.); reyes@ictp.csic.es (R.V.-M.); sergio@ictp.csic.es (S.G.); r.verdejo@csic.es (R.V.); lmanchado@ictp.csic.es (M.A.L.-M.)

* Correspondence: marherna@ictp.csic.es



Citation: Araujo-Morera, J.; Verdugo-Manzanares, R.; González, S.; Verdejo, R.; Lopez-Manchado, M.A.; Hernández Santana, M. On the Use of Mechano-Chemically Modified Ground Tire Rubber (GTR) as Recycled and Sustainable Filler in Styrene-Butadiene Rubber (SBR) Composites. *J. Compos. Sci.* **2021**, *5*, 68. <https://doi.org/10.3390/jcs5030068>

Academic Editor:
Francesco Tornabene

Received: 5 February 2021
Accepted: 26 February 2021
Published: 3 March 2021

Publisher's Note: MDPI stays neutral with regard to jurisdictional claims in published maps and institutional affiliations.



Copyright: © 2021 by the authors. Licensee MDPI, Basel, Switzerland. This article is an open access article distributed under the terms and conditions of the Creative Commons Attribution (CC BY) license (<https://creativecommons.org/licenses/by/4.0/>).

Abstract: The management of end-of-life tires (ELTs) is one of the main environmental issues that society faces nowadays. Recycling of ELTs appears as one feasible option for tackling the problem, although their incorporation as ground tire rubber (GTR) in other rubber matrices is limited due to poor compatibility. In this research, we report a successful combination of a cryo-grinding process with a chemical treatment for modifying the surface of GTR. Various cryo-grinding protocols were studied until a particle size of 100–150 µm was achieved. Chemical treatments with different acids were also analyzed, resulting in the optimal modification with sulfuric acid (H₂SO₄). Modified GTR was added to a styrene-butadiene rubber (SBR) matrix. The incorporation of 10 phr of this filler resulted in a composite with improved mechanical performance, with increments of 115% and 761% in tensile strength and elongation at break, respectively. These results validate the use of a recycled material from tire waste as sustainable filler in rubber composites.

Keywords: circular economy; sustainability; recycling; ground tire rubber; surface treatment; chemical modification; styrene-butadiene rubber

1. Introduction

The rational use of raw materials and polymer waste management, especially end-of-life tires (ELTs), is a global problem. One possible solution to this disposal issue is to recycle the waste and reuse it. Recycling of resources and products is one of the main strategies of the circular economy (CE) model, providing an alternative to the traditional linear economy. The CE model aims to take care of the environment and achieve a sustainable society, keeping resources in use for as long as possible and reducing costs and waste [1]. By using recycled rubber, it is possible to give a second lifecycle to a considerable number of used tires.

The first stage in any tire recycling route should involve the consideration of the production of ground tire rubber (GTR), a fine granular material obtained from worn tires. The grinding is generally carried out by impact, shearing, or cutting actions under various environmental conditions, transforming the used tires into a powder of the desired particle size. Dry or wet ambient mechanical grinding and cryogenic grinding are some of the various methods used to obtain GTR [2,3].

Direct recycling options for GTR cover a wide variety of successful applications. The use of GTR in the cement and concrete industry is an area of research that has developed considerably in the last decades [4]; in this application, the GTR improves fracture resistance, decreases density, favors thermal and acoustic isolation properties, and reduces the transmission of crack and vibrations. Also, the asphalt industry uses GTR as filler for treating road surfaces [5,6] since it reduces the noise generated by vehicles, improves crack

and skid resistance, provides a more comfortable ride, and enhances road performance and longevity.

GTR can also be incorporated into thermosets [7–10] and thermoplastics [11–13] as a toughening agent and into virgin rubber as a semi-active filler [14–21]. However, its use in rubber has been, up to now, restricted to the production of technically less demanding goods, since the low compatibility with the matrix is a major issue. In general, the direct incorporation of GTR in rubber composites significantly deteriorates the viscoelastic and physical properties, compared to the virgin composites. This behavior is due to the weak matrix-filler adhesion, which leads to poor mechanical properties even at low contents. The complex three-dimensional network molecular structure of GTR limits the molecular interactions with the polymeric matrix, reducing their compatibility.

Surface treatments appear to be a valid approach for improving the bonding, and consequently the compatibility, between GTR and any polymeric matrix [22]. Surface functionalization of GTR can be carried out with several physical methods, such as plasma [23–25], ozone [26,27], high-energy gamma [28], or ultraviolet (UV) [29] irradiation. Chemical methods such as acids [30–34], coupling agents [35,36], and chlorination reactions [37] can also be used. All these different treatments aim to modify the surface, generating polar groups derived from oxidation—such as carbonyl, hydroxyl or peroxy groups—or through chemical etching and even partial devulcanization. Chemical acid treatment has been reported as one of the most successful surface modification reactions since it generates a porous GTR surface. Some examples have been reported previously in thermoplastics matrices [31–34] but it is not as widely used in rubber matrices. As an example, Yehia et al. [30] prepared natural rubber (NR) composites filled with chemically modified GTR and in combination with carbon black (CB). The modification of the GTR was carried out with different concentrations of nitric acid (HNO_3) and 30% hydrogen peroxide (H_2O_2) solution. The authors found that the tensile strength was improved with treated GTR (40 phr). The highest tensile strength values were obtained with 20% HNO_3 (45%) and 30% H_2O_2 (63%) solutions. Furthermore, they found that the incorporation of up to 20 phr of GTR in combination with the CB led to the retention of at least 50% of its physico-mechanical properties before and after aging.

In this article, we present a successful combination of a mechanical process (cryogrinding) and a chemical modification (acid treatment) for the modification of the surface of GTR that can achieve excellent mechanical properties in styrene-butadiene rubber (SBR)/GTR composites with only 10 phr of GTR. We analyzed several cryogrinding protocols, varying grinding time and the number of cycles, and studied different chemical reactions by using H_2O_2 , sulfuric acid (H_2SO_4), HNO_3 , and a combination of $\text{H}_2\text{SO}_4/\text{HNO}_3$. This effective mechano-chemical procedure can be considered a novel and optimal approach for incorporating a recycled material as sustainable filler in rubber matrices with improved interfacial adhesion.

2. Materials and Methods

2.1. Materials

Arlanxeo (Maastricht, The Netherlands) kindly supplied styrene-butadiene rubber (SBR) (BUNA SE1502H). Ground tire rubber (GTR), obtained by ambient grinding (a blend of truck and passenger car tires), was kindly supplied by Signus Ecovalor (Madrid, Spain). The average particle size of the as-received GTR was 1000 μm . The as-received GTR showed an average composition of 55 phr NR, 45 phr SBR/polybutadiene rubber (BR) and 50 phr carbon black. The composition of the as-received GTR and the relative proportions of rubber, carbon black, and ash content were determined by thermogravimetric analysis (TGA). The full characterization of the as-received GTR has been reported previously [17]. Sulfuric acid (H_2SO_4 ; 95–98% pure, pharma grade) and hydrogen peroxide (H_2O_2 ; 33% w/v stabilized pure, pharma grade) were supplied by PanReac AppliChem (PanReac AppliChem, Barcelona, Spain). Nitric acid (HNO_3 ; 69% for analysis) was supplied by

Merckmillipore (Merckmillipore, Darmstadt, Germany). Commercial grade vulcanizing additives were used as received.

2.1.1. Grinding Protocols

The as-received GTR was further pulverized under cryogenic conditions using a Cryomill (Retsch, Hann, Germany) with three different grinding protocols, varying the number of cycles and grinding time (Table 1) to reduce the particle size.

Table 1. Grinding protocols varying number of cycles and grinding time.

Grinding Protocol	Number of Cycles	Grinding Time (min)	Intermediate Cooling (min)	Total Time (min)
P1	18	2	1	54
P2	27	1	1	54
P3	36	0.5	1	54

2.1.2. Surface Modification of GTR

GTR, cryoground according to the optimum grinding protocol, was chemically modified with different oxidizing agents (H_2SO_4 , HNO_3 , and H_2O_2). A total of 10 g of GTR was placed in a 1000 mL round-bottom flask in an ice bath, and then the oxidizing agent was introduced dropwise with continuous magnetic stirring until complete immersion of the GTR. The mixtures were heated to 100 °C over 3 h for the H_2SO_4 , HNO_3 , and the H_2SO_4/NHO_3 mixture (in a 3:1 ratio), and at room temperature for H_2O_2 , in order to avoid the early decomposition of the oxidizing agent and to guarantee the full reaction between the GTR and H_2O_2 ; all procedures utilized magnetic stirring. The modified GTR (m-GTR) was washed thoroughly with purified water at room temperature until a neutral pH solution was obtained. All the materials were dried in an oven at 70 °C for 24 h.

2.1.3. Composites Preparation

Rubber composites were developed according to the compositions shown in Table 2.

Table 2. Formulations of styrene-butadiene rubber (SBR) composites. ZnO: zinc oxide, SA: stearic acid, CBS: N-cyclohexylbenzothiazole-2-sulfenamide, S: sulfur, GTR: ground tire rubber (cryo-ground GTR), m-GTR: modified ground tire rubber.

Composite	Ingredient (phr)						
	SBR 1502	ZnO	SA	CBS	S	GTR	m-GTR
Unfilled	100	5	1	1	1	-	-
10 GTR	100	5	1	1	1	10	-
20 GTR	100	5	1	1	1	20	-
30 GTR	100	5	1	1	1	30	-
10 m-GTR	100	5	1	1	1	-	10
20 m-GTR	100	5	1	1	1	-	20
30 m-GTR	100	5	1	1	1	-	30

The mixing was carried out in a two-roll open mill (MGN-300S, Comerio Ercole, Busto Arsizio VA, Italy) using a rotor speed ratio of 1:1.5 at room temperature. Rubber was passed through the rollers until a band was formed. The activating complex—ZnO and SA—GTR and the curatives—CBS and S (Sigma Aldrich, St. Louis, MO, USA)—were sequentially added to the rubber.

The crosslinking process was monitored by checking the torque variation as a function of time using a Rubber Process Analyzer (RPA2000, Alpha Technologies, Akron, OH, USA) at a frequency of 0.833 Hz and with 2.79% strain over 300 min at the curing temperature $T_c = 160$ °C. Then, the compounds were vulcanized in an electrically heated hydraulic

press (Gumix, Barcelona, Spain) at 160 °C and 20 MPa according to their optimum curing time t_{90} derived from the curing curves data.

2.2. Characterization

2.2.1. Particle Size Distribution

GTR powder (~0.05 g) was previously dispersed in 20 mL of a water/ethanol 70/30 solution with 0.2 mL of surfactant Triton X-100. The suspension was sonicated in an ultrasound bath (Elmasonic S40H, Corroios, Portugal) for about 2 h. The particle size distribution was obtained by means of a laser scattering particle size distribution analyzer (Coulter LS 200, CA, USA). A volume standard cumulative distribution was measured under stabilized conditions. Each sample was subjected to a 60 s optical measurement.

2.2.2. Hydrophilicity Test

GTR powder (~1 g) was mixed with 10 mL of water. The mixture was stirred for 10 min. Pictures were taken to analyze the dispersion and hydrophilic nature of the powder

2.2.3. Fourier-Transform Infrared Spectroscopy

The changes in the functional groups produced by the modification process were studied by infrared spectroscopy (PerkinElmer spectrometer UATR Two, Waltham, MA, USA) from 400 to 4000 cm^{-1} with a resolution of 4 cm^{-1} in the ATR mode. The measurements were performed directly on the GTR powder.

2.2.4. X-ray Photoelectron Spectroscopy

X-ray photoelectron measurements were performed on the surfaces of as-received GTR, cryo-ground GTR (GTR Cryo), and modified GTR (m-GTR) using a spectrometer (MT500, Fisons Instruments, East Grinstead, UK) equipped with a hemispherical electron analyzer (CLAM 2) and an Mg Ka X-ray source (1253.6 eV) operated at 300 W. Binding energies were corrected to the carbon 1s peak located at 285 eV.

2.2.5. Scanning Electron Microscopy

The samples were cryogenically broken in liquid nitrogen and the fractured ends of the specimens were sputter-coated with gold. The morphology of the samples was analyzed by means of an environmental scanning electron microscope (SEM, XL30, Philips, Amsterdam, The Netherlands) with a tungsten filament with an acceleration voltage of 25 kV.

2.2.6. Energy Dispersive X-ray Spectroscopy

The samples were analyzed by means of a high-resolution scanning electron microscope (S-8000, Hitachi, Tokyo, Japan) with a tungsten filament with an acceleration voltage of 15 kV.

2.2.7. Tensile Measurements

Dogbone-shaped samples were used for uniaxial tensile testing. Tests were performed on a universal mechanical testing machine (Instron 3366, Grand Rapids, MI, USA) equipped with a 1 kN load cell. Samples were stretched until failure at a constant crosshead speed of 200 mm/min at room temperature.

2.2.8. Cross-Link Density

Cross-link density was determined from the measurements of solvent-swelling in toluene, applying the Flory-Rehner [38] equation and assuming the formation of tetra-functional cross-links during the vulcanization reaction. For each rubber composite, five samples were cut from rubber sheets of approximately 2 mm thickness and were weighed and immersed in toluene at ambient temperature for a period of 72 h. After this time, the samples were blotted with filter paper to remove the excess of solvent and immediately

weighed. Finally, the test samples were dried in a vacuum oven for 24 h at 60 °C. The cross-link density was calculated according to the following equations:

$$v \left(\frac{\text{mol}}{\text{cm}^3} \right) = \frac{\rho_r}{2Mc} = - \frac{\ln(1 - V_r) + V_r + \chi V^2}{2V_s \left(V_r^{1/3} - \frac{V_r}{2} \right)} \quad (1)$$

where Mc is the average molecular weight of the rubber between the cross-links, V_r is the volume fraction of the equilibrium swollen rubber, χ is the Flory-Huggins polymer–solvent interaction parameter, ρ_r is the density of rubber (g/cm^3), and V_s is the molar volume of the solvent used ($106.27 \text{ cm}^3/\text{mol}$ for toluene). The V_r was determined from Equation (2).

$$V_r = \frac{\frac{w_d}{\rho_r} - V_f}{\frac{w_d}{\rho_r} - V_f + \frac{w_s - w_d}{\rho_s}} \quad (2)$$

where w_d is the weight of the dried sample after evaporation of the solvent, w_s is the swollen weight of the sample, ρ_s is the solvent density ($0.867 \text{ g}/\text{cm}^3$ for toluene), and V_f is the volume fraction of insoluble materials in the rubber composite recipe, determined with Equation (3).

$$V_f = f \frac{w_i}{\rho_r} \quad (3)$$

where w_i is the initial weight of the sample before swelling and f is the fraction of insoluble materials of the composite recipe, determined from Equation (4)

$$f = \frac{w_{ins}}{w_r} \quad (4)$$

where w_{ins} is the weight of insoluble materials in the composite and w_r is the total weight of the composite recipe. In this research, GTR was considered as the insoluble fraction in all composites.

2.2.9. Dynamic-Mechanical Analysis

Dynamic-mechanical analysis (DMA) spectra were registered using a DMA Q800 device (TA Instruments, New Castle, DE, USA). Dogbone specimens were tested in tensile mode at a static preload of 0.1 N with a superimposed sinusoidal of 0.2% strain. The spectra were taken in a temperature range of -100 to 160 °C at a frequency of 1 Hz. The temperature ramp was 2 °C/min.

The interfacial interactions between SBR and GTR can be calculated with the adhesion factor (A) from the loss factor ($\tan\delta$) using the following equation [39]:

$$\frac{\tan \delta_c}{\tan \delta_r} \cong (1 - V_f)(1 + A) \quad (5)$$

where $\tan\delta_r$ is the loss tangent of the unfilled SBR, $\tan\delta_c$ the loss tangent of the SBR-GTR composite, and V_f is the volume fraction of the filler phase.

3. Results and Discussion

3.1. Mechano-Chemical Modification of GTR

3.1.1. Particle Size Distribution

As seen in Figure 1 and Table 3, all of the cryo-grinding protocols used significantly reduced the average particle size of as-received GTR, decreasing it from $1000 \mu\text{m}$ to $100\text{--}150 \mu\text{m}$. Although there does not seem to be a considerable difference between the three protocols, protocol P1 resulted in a narrower particle size distribution. Hence, protocol P1 was selected as the optimized cryo-grinding method.

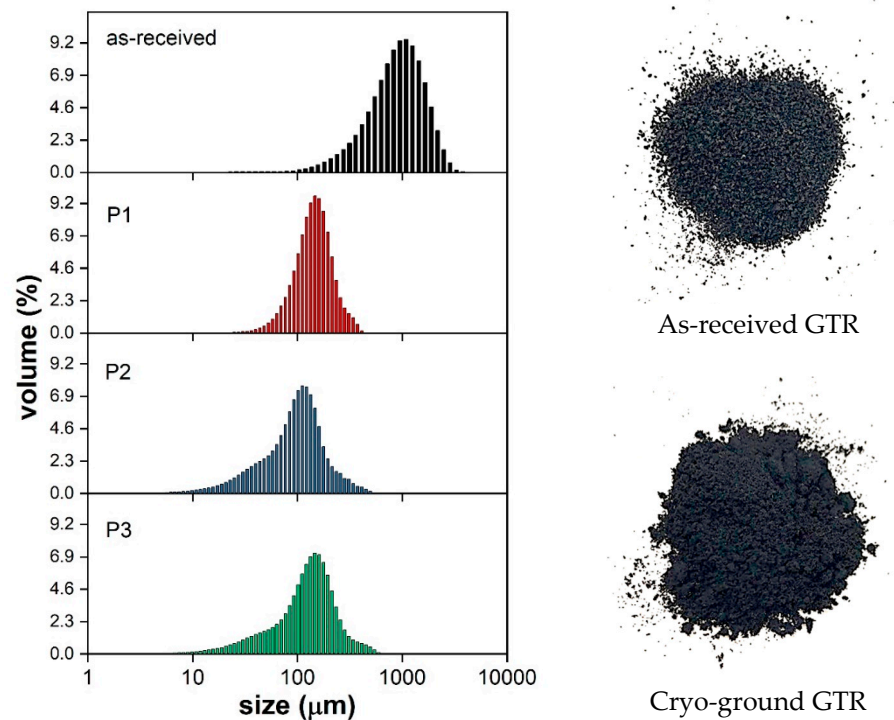


Figure 1. Particle size distribution of as-received and cryo-ground ground tire rubber (GTR) according to different grinding protocols.

Table 3. Average particle size and diameter, on cumulative percentage, of the as-received and cryo-ground GTR according to different grinding protocols.

Grinding Protocol	Average Particle Size (μm)	Diameter on Cumulative Percentage (μm)		
		10	50	90
As-received	1043	288	744	1439
P1	153.8	81	145	236
P2	115.0	33	99	171
P3	147.1	42	135	254

3.1.2. Surface Modification of GTR

When the cryo-ground GTR (GTR Cryo) was chemically modified (m-GTR), the average particle size decreased, especially for the oxidizing treatments with H₂SO₄, HNO₃, and their mixture, as seen in Figure S1 and Table S1 (Supplementary Information SI). In addition, the particle size distribution became wider, which is evidence of the irregular surface modification.

Figure 2 shows SEM micrographs of the surfaces of all GTR samples at 500× magnification. The as-received GTR shows a large, cracked, and irregular surface with a rough texture, which is characteristic of tire powders ground under ambient temperature conditions [34]. The cryo-grinding process generates a different morphology, showing a smoother fracture surface due to the brittle failure mechanism. Moreover, the cryo-ground GTR (GTR Cryo) presents a smaller particle size that is homogeneously distributed [3]. Microcavities and micropores can be seen in the modified GTR (m-GTR). These irregularities can be considered to be the result of the strong attacks of oxidizing agents, which are able to degrade and remove some chemical components of the GTR particles, such as additives and waxes. Also, some sphere-shaped particles can be observed at the surface of the treated GTR, which may relate to zinc oxide, silica, and carbon black added to the tire formulation [34]. As an illustrative example, Figure 3 shows the energy dispersive X-ray

(EDX) elemental mapping of the m-GTR sample treated with H_2SO_4 at $150\times$ magnification. One can see that the elements C, O, S, and Zn are uniformly distributed in the composite. Furthermore, one can infer that the major proportion of spherical particles corresponded to Si. The new morphology of m-GTR may improve interfacial adhesion with the SBR matrix and, thus, its dispersion since the formation of microcavities and pores could significantly increase the surface area and, therefore, its interfacial contact with the matrix [33,40].

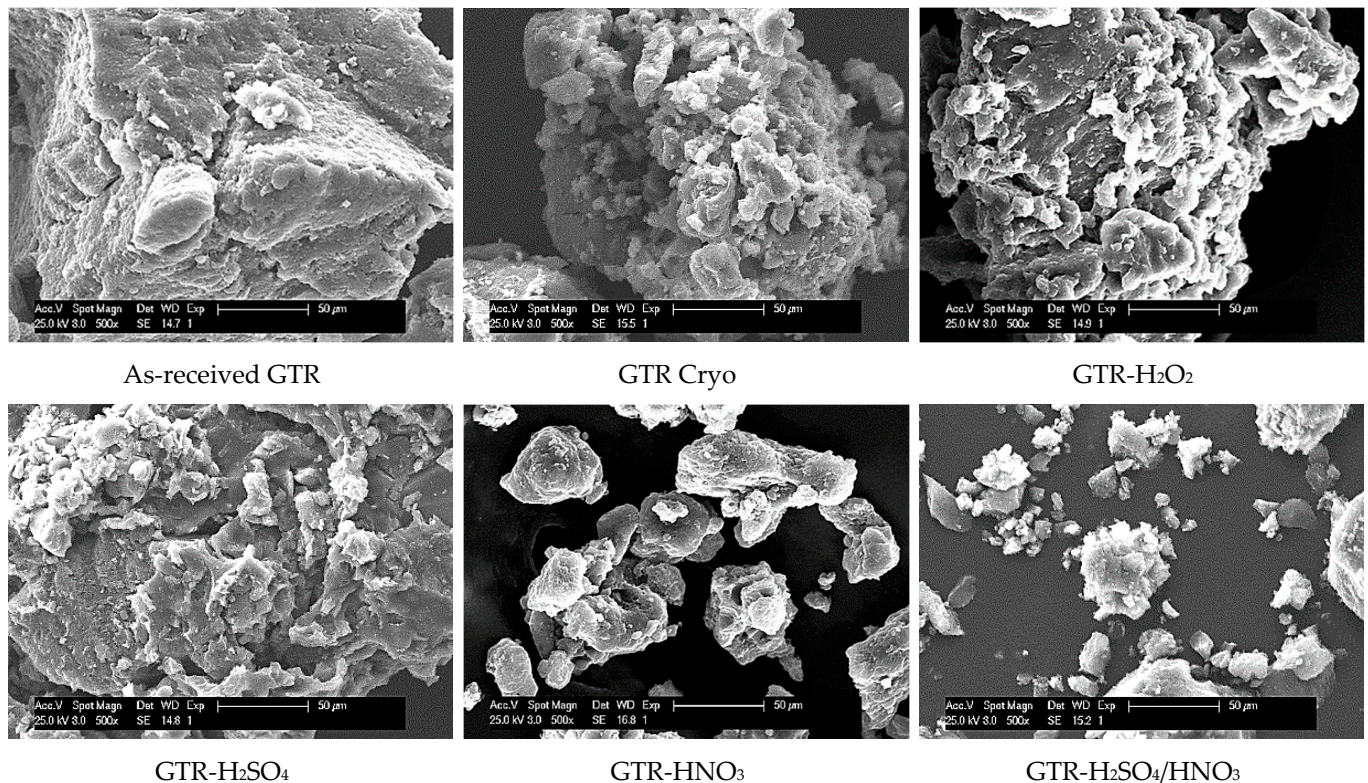


Figure 2. Scanning electron microscope (SEM) micrographs of GTR and modified GTR (m-GTR) with different treatments at a magnification of $500\times$.

The Fourier-transform infrared (FTIR) spectroscopy analysis was used to learn about the structure and functional groups present in the m-GTR and to compare the effects of the different oxidizing treatments. Figure 4 shows the respective characteristic vibrations of GTR before and after the chemical treatments. As-received and cryo-ground GTR showed signals at 2920 and 2850 cm^{-1} , which can be ascribed to the stretching of C-H. After the chemical treatments, these bands decreased in intensity and new absorption bands were detected; $\text{C}=\text{C}$ at 1640 cm^{-1} and carbonyl groups ($\text{C}=\text{O}$) at 1720 cm^{-1} . The presence of these carbonyl groups is frequently correlated to hydroxyl groups (OH). The characteristic broad absorption band at 3440 cm^{-1} , corresponding to the stretching vibration of the OH group, resulted from the oxidation processes, showing a more intense signal when GTR was treated with H_2SO_4 and HNO_3 . A strong band corresponding to C-O stretching was also observed at 1100 cm^{-1} for the m-GTR chemically treated with HNO_3 . Additionally, in the case of the chemical treatment with the H_2SO_4/HNO_3 mix, two peaks in the $1000\text{--}1200\text{ cm}^{-1}$ region are indicative of the $\text{O}=\text{S}=\text{O}$ stretching [34]. These new chemical groups grafted onto the surface of m-GTR could improve the interfacial adhesion with different polymer matrices. These functional groups increase the polarity on the surface of the GTR and, therefore, may increase its reinforcing efficiency due to potential chemical reactions with other suitable functional groups present in the reaction medium [30]. These findings fit well with the results of the hydrophilicity test, as described below.

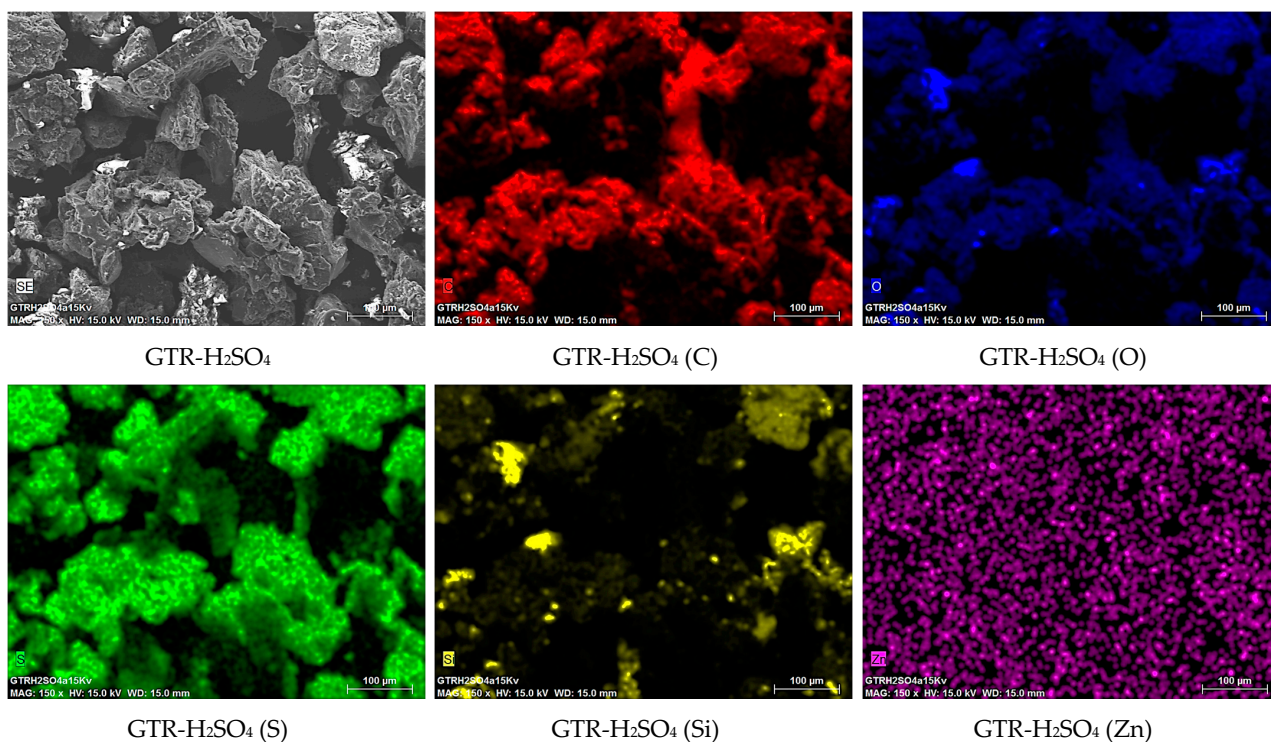


Figure 3. Energy dispersive X-ray (EDX) elemental mapping of m-GTR sample treated with H₂SO₄ at a magnification of 150×.

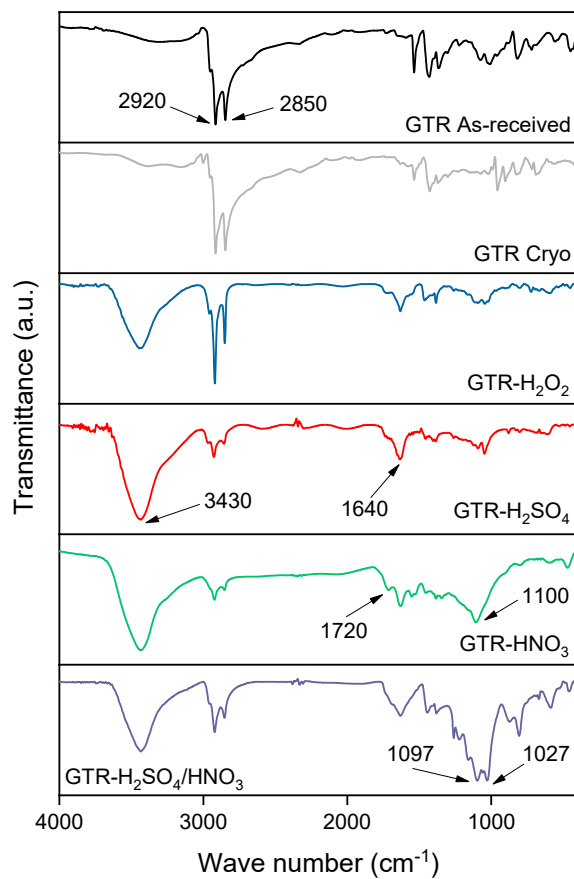


Figure 4. Fourier-transform infrared (FTIR) spectra of as-received, cryo-ground (GTR Cryo), and chemically treated GTR.

Figure 5 shows that the as-received, cryo-ground, and H_2O_2 modified GTR were completely hydrophobic, evidenced by the suspension of the GTR particles on the water after stirring. This fact can be attributed to the non-polar nature of the untreated GTR, which prevents its interaction with water. After the chemical modification with H_2SO_4 , HNO_3 , and $\text{H}_2\text{SO}_4/\text{HNO}_3$, m-GTR dispersed uniformly in the water, corroborating the compatibility between the treated GTR and the aqueous medium. The chemical treatment induced a polarity on the surface of the m-GTR that enabled electrostatic interactions with the water.

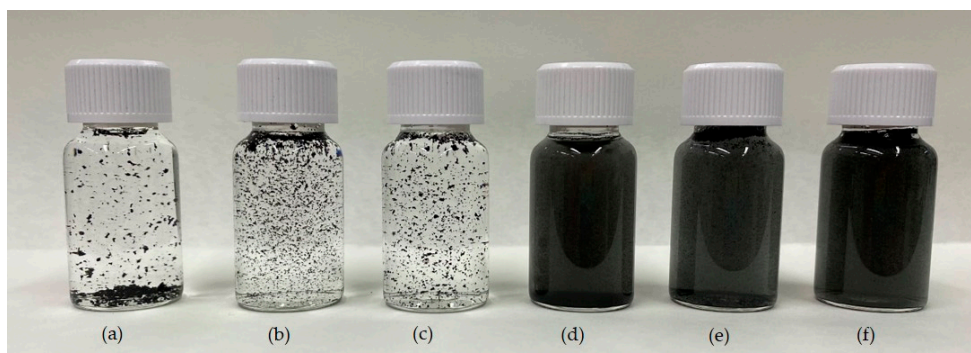


Figure 5. Hydrophilic behavior of (a) as-received, (b) cryo-ground, (c) H_2O_2 -modified, (d) H_2SO_4 -modified, (e) HNO_3 -modified, and (f) $\text{H}_2\text{SO}_4/\text{HNO}_3$ -modified GTR.

X-ray photoelectron spectroscopy (XPS) analysis was also used to detect variations on the GTR surface after the chemical treatments. Figure 6 shows the C 1s (left-side figures) and O 1s (right-side figures) core spectra of unmodified and chemically modified GTR. The C 1s core spectra of as-received GTR (Figure 6a) and GTR Cryo (Figure 6c) show peaks at 284.5 eV (C=C) and 285 eV (C-H) and a very small peak at 286.5 eV (C-OH). The main component at 285 eV was the result of the similarity of carbon surroundings, which remained practically unaltered. This suggests that most of the carbon atoms were of the same nature. After being chemically treated, GTR- H_2SO_4 (Figure 6e) showed a shift of the C 1s excitation to higher energy due to the presence of oxygen-containing groups. This spectrum is representative of all chemical treatments carried out. The same trend was observed for the other chemical treatments presented in Figure S2 (Supplementary Information S1). Two new peaks appeared at the 287.6 and 288.9 eV binding energies, which can be assigned to the C=O and HO-C=O species, respectively, on the CB surface and/or on polymer chains generated by oxidation during the chemical treatments. The C-H bonds of GTR were disrupted, resulting in the dehydrogenation and generation of free radicals. Due to their reactive nature, these radicals can react with oxygen and water in the atmosphere to form peroxide and hydroxyl peroxide species. The introduction of the oxygen-containing polar functional groups onto the GTR surfaces corresponded to the increase in surface energy [41].

The O 1s core spectra are shown in Figure 6b,d,f. They can be deconvoluted into two peaks, showing the combination of oxygen and carbon with both double (O=C) and single (O-C) bonds, at 530 eV and at 532.4 eV, respectively. In all cases, the peak height of O 1s increased after the oxidizing treatment. From these results, one can confirm that the GTR surface was successfully modified with oxygen.

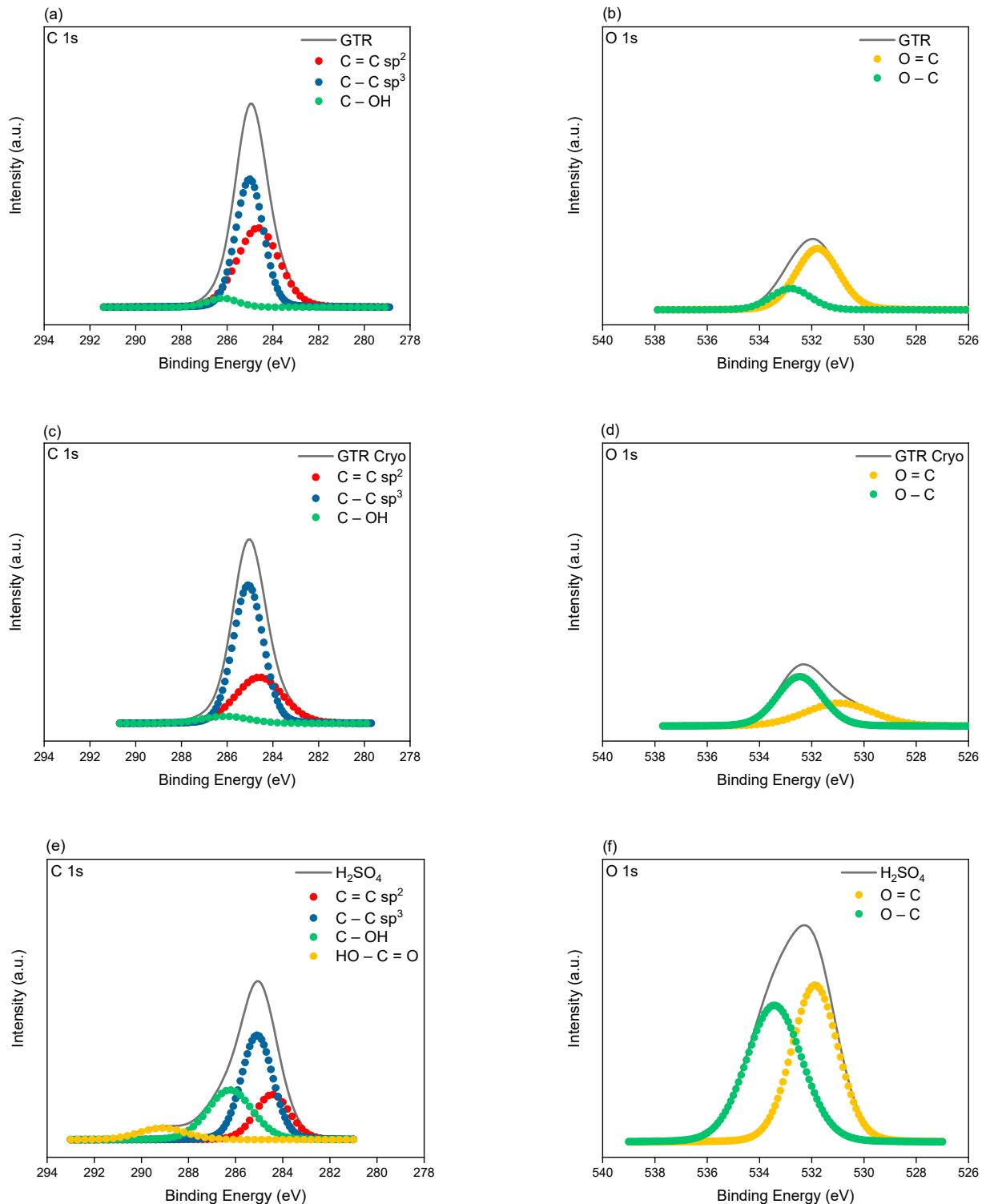


Figure 6. C and O core spectra of: (a) and (b) as-received GTR; (c) and (d) GTR Cryo; (e) and (f) GTR modified with H₂SO₄.

The surface composition determined through the XPS of the as-received GTR and after chemical treatment is summarized in Table 4. Sulfur (S), oxygen (O), silicon (Si), and nitrogen (N) elements were present in different amounts depending on the chemical modification. The as-received and cryo-ground GTR showed subtle changes in their composition. The existence of a lower amount of O in as-received GTR and in GTR Cryo would be reasonable due to carbonate additives and metal oxides; moreover, the presence of O in modified samples was directly related to the various oxidation treatments. The O

content on the surface of all the chemically treated GTR rose due to the oxidation process, increasing by 3.5%, 10.1%, 11.2%, and 14.3% for the H₂O₂, HNO₃, H₂SO₄/HNO₃, and H₂SO₄ treatments, respectively, compared to cryo-ground GTR. In addition, one can infer that the S contribution came from the vulcanization process and, in a higher proportion, from the H₂SO₄ treatment. However, the GTR-H₂O₂ did not show the S content as would be expected. No significant change in silicon (Si) content could be observed. Moreover, from the XPS study, one can analyze the O/C ratio as another interesting parameter. From the values compiled in Table 4, one can notice that the O/C ratio increased, which might have been induced by increasing –OH groups on the material surface after the oxidizing treatment. This proven oxidization reaction occurred between the oxidizing agents and the surface molecules in GTR, introducing oxygen onto the GTR surface. The ratio of O/C increased to 0.133, 0.233, 0.251, and 0.315 for the H₂O₂, HNO₃, H₂SO₄/HNO₃, and H₂SO₄ treatments, respectively.

Table 4. Analysis of GTR samples by X-ray photoelectron (XPS) (surface relative element content) and EDX spectroscopy.

	As-received GTR	GTR Cryo	GTR-H ₂ O ₂	GTR-H ₂ SO ₄	GTR-HNO ₃	GTR-H ₂ SO ₄ /HNO ₃
XPS Analysis						
Element	Normalized Content (%)					
C	91.12	90.19	86.13	73.02	79.61	78.31
O	6.95	7.93	11.46	23.01	18.52	19.69
S	0.67	0.47	-	2.70	0.35	2.97
Si	1.25	1.41	2.40	1.28	1.51	1.43
O/C	0.076	0.088	0.133	0.315	0.233	0.251
EDX Analysis						
Element	Normalized Content (wt%)					
C	82.97	81.58	82.71	68.88	79.39	85.58
O	8.71	10.08	10.64	21.82	16.30	11.56
S	1.95	1.68	1.56	7.26	0.75	0.67
Si	1.21	0.73	1.08	1.62	3.23	1.94
Mg	0.06	0.10	0.05	0.02	0.03	0.06
Al	0.18	0.12	0.14	0.10	0.12	0.18
Ca	0.55	0.25	0.06	0.04	0.01	0
Fe	1.59	2.60	1.63	0.09	0.15	0.01
Zn	2.78	2.86	2.13	0.17	0.02	0

To further confirm the modification of GTR, we used EDX spectroscopy as an analytical method for determining the element composition. According to the results compiled in Table 4, all samples contain C, O, Si, S, Fe, and Zn. The as-received GTR, GTR Cryo and GTR modified with H₂O₂ had the same composition. Despite there being a slight variation in the case of the modification carried out by H₂SO₄/HNO₃, the same trend was observed for the two techniques (XPS and EDX). After the chemical treatment, the O content increased due to the oxidation reaction, with the GTR modified with H₂SO₄ presenting the major proportion of oxygen. Thus, this filler (GTR-H₂SO₄) was selected for further research, adding it to SBR compounds, as discussed in the following section.

3.2. Characterization of SBR–GTR Composites

3.2.1. Physico-Mechanical Properties

Figure 7 shows the vulcanization curves obtained for SBR composites filled with GTR and m-GTR. The most notorious characteristic is revealed by the m-GTR composites presenting a marching modulus behavior. This behavior is characterized by torque that does not level out but continues to rise. The effect of GTR and m-GTR on the vulcanization process parameters can be analyzed from the values shown in Table 5. The minimum torque (ML) slightly increased with increasing GTR and m-GTR content. This behavior

indicates that the incorporation of the filler into the compound hindered the processing. This behavior may be associated with the agglomeration of tire waste particles in the matrix. A drop in the maximum torque (MH) as well as in the delta torque ($\Delta M = MH - ML$) can be seen. Such a trend can be attributed to the migration of sulfur from the elastomeric matrix towards the vulcanized GTR particles, resulting in a lower crosslinking degree [15]. Moreover, unreacted crosslinking precursor fragments (accelerators and activators) in the vulcanized waste can migrate towards the virgin matrix. Hence, scorch time (t_{s2}) and optimum vulcanization time (t_{90}) decreased with the increment in GTR content, indicating that the crosslinking reactions started earlier. Similar behavior has been reported by other authors, confirming the effect of the curatives on the rheometric properties of rubber matrices filled with GTR [15,16,42]. Furthermore, it is possible that, for higher filler content, the curatives diffusion rate within the matrix decreases, resulting in an increase in the t_{90} [23]. However, in the case of the composites filled with m-GTR, the scorch time increased due to the characteristic marching modulus behavior. An analogous behavior can be seen in silica-filled composites [43]. The adsorption of the accelerator (CBS) on the silica surface can explain the slower cure characteristics. The high content of acid hydroxyl groups means that these groups can easily form hydrogen bonds between polar materials, especially basic organics, and silica. Moreover, the sulfur linkages and amine group of CBS can form hydrogen bonds with the hydroxyl groups of silica. This can weaken the strength of the N-S bonds of CBS and accelerate their dissociation. This effect is more pronounced with higher silica content. Therefore, the increased adsorption of CBS can explain the slower cure characteristics. In a similar way, in this research the m-GTR particle surface was acidic, due to the presence of hydroxyl groups, and thus tended to bond to and deactivate the accelerator molecules.

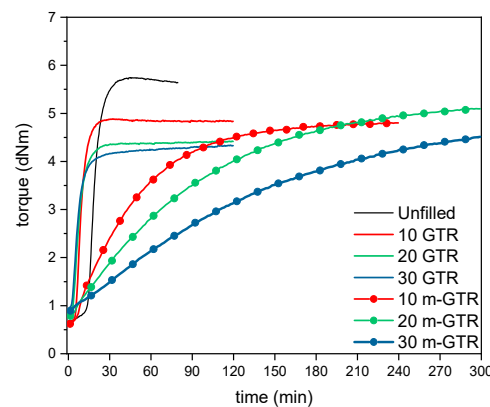


Figure 7. Rheometric curves of SBR, SBR-GTR, and SBR-m-GTR composites.

Table 5. Rheometric properties of SBR-GTR and SBR-m-GTR composites.

Composite	ML (dNm)	MH (dNm)	ΔM (dNm)	t_{s2} (min)	t_{90} (min)
Unfilled	0.7	5.8	5.1	17	27
10 GTR	0.6	4.9	4.3	9	15
20 GTR	0.8	4.4	3.6	8	16
30 GTR	1	4.4	3.4	8	18
10 m-GTR	0.6	3.6	3	34	52
20 m-GTR	0.8	3.8	3	57	82
30 m-GTR	0.9	3.9	3	100	136

In an attempt to fix a realistic curing time and limit the marching trend of the m-GTR-filled composites, the variation of torque, ΔM , was established as a fixed parameter. The maximum torque, MH, and the time (t_{s2} and t_{90}), shown in Table 5, were associated with this value. It is well-known that ΔM can be considered as an indirect measure of the

cross-link density of a rubber composite. Nonetheless, different cross-link values were obtained for the three m-GTR-filled composites. This unexpected behavior can be ascribed to the uncontrolled migration of sulfur from the SBR matrix to the m-GTR, reducing the cross-link density. This effect is especially notorious with regard to the increment in the chemically modified GTR content. Hence, it is challenging to control the cross-link density in rubber composites filled with chemically modified GTR (m-GTR).

Table 6 summarizes the physico-mechanical properties of the vulcanized composites. The incorporation of cryo-ground GTR and m-GTR decreased the cross-link density of the SBR composites. The lower level of crosslinks in the rubber matrix may be attributed to the relatively fewer reaction sites available for additional crosslinking after the addition of the GTR [44]. Hardness and resilience values decrease, correspondingly; with SBR-m-GTR composites showing a more noticeable effect. The hardness of rubber composites deeply depends on filler properties, such as particle size and surface characteristics, and on the cross-link density of the rubber composite. The functional groups present on the m-GTR surface and the acid–base interactions lead to the formation of m-GTR particle aggregates and to a decrease in the cross-link density of the SBR matrix. This aggregation decreases the availability of surface functional groups to improve the physical bonding between the m-GTR and the SBR matrix. Thus, it leads to a decrease in the hardness of rubber [45].

Table 6. Physico-mechanical properties of cryo-ground GTR-SBR and m-GTR-SBR composites.

Composite	Unfilled (SBR)	10 GTR	20 GTR	30 GTR	10 m-GTR	20 m-GTR	30 m-GTR
M_{50} (MPa)	0.52 ± 0.02	0.57 ± 0.04	0.5 ± 0.1	0.63 ± 0.03	0.52 ± 0.03	0.59 ± 0.03	0.58 ± 0.04
M_{100} (MPa)	0.67 ± 0.02	0.69 ± 0.01	0.6 ± 0.1	0.66 ± 0.03	0.62 ± 0.03	0.60 ± 0.03	0.6 ± 0.1
M_{300} (MPa)	0.97 ± 0.02	0.97 ± 0.01	0.8 ± 0.1	0.93 ± 0.02	0.75 ± 0.03	0.80 ± 0.02	0.81 ± 0.04
M_{500} (MPa)	1.33 ± 0.4	1.37 ± 0.02	1.3 ± 0.1	1.26 ± 0.02	0.94 ± 0.03	1.05 ± 0.02	1.08 ± 0.01
σ_b (MPa) P	1.4 ± 0.1	2.0 ± 0.1	2.5 ± 0.2	2.0 ± 0.1	2.8 ± 0.2	2.49 ± 0.02	2.0 ± 0.1
ϵ_b (%)	521 ± 18	732 ± 23	1016 ± 112	1017 ± 84	1187 ± 146	1305 ± 94	1388 ± 15
$\nu \times 10^{-6}$ (mol/cm ³)	22.7 ± 0.3	14.3 ± 0.2	6.4 ± 0.2	3.8 ± 0.1	6.5 ± 0.1	3.8 ± 0.1	2.4 ± 0.1
Hardness (Shore A)	34	31	31	31	27	27	31
Resilience (%)	65	61	59	56	62	62	61

The effect of the GTR and m-GTR contents and surface modification of GTR on the mechanical behavior of SBR vulcanizates can also be analyzed from the values compiled in Table 6. The M_{50} , M_{100} , M_{300} , and M_{500} values correspond to the tensile stress at 50%, 100%, 300%, and 500% strain, respectively. The σ_b and ϵ_b values correspond to tensile strength and elongation at break, respectively. At deformations up to 500%, the GTR and m-GTR did not seem to have an effect on the mechanical response of the material. However, the effect on elongation at break and tensile strength is noticeable. Elongation at break increased significantly with the increment of filler content, about 262% for GTR and 712% for m-GTR with 10 phr of filler. This notorious elongation at break is consistent with the evident reduction of the cross-link density. Tensile strength also increased in the presence of GTR and m-GTR, the effect being more evident with the chemically modified material at lower contents. Increments of 54% and 115% with 10 phr of GTR and m-GTR can be observed. At higher contents of GTR and m-GTR, filler–filler interactions can be favored, forming a filler network in the rubber system that reduces its reinforcement effect. Similar results were reported by Dai et al. [46]. They found that chemically modified CB-filled composites showed higher tensile strength but similar elongation at break values compared with unmodified CB-filled composites. In another study, Zhang et al. [41] modified GTR with plasma treatment to improve the adhesion with a nitrile rubber (NBR) matrix. The increased interfacial bonding between the plasma-modified GTR and the rubber matrix improved the tensile strength while the elongation at break remained unchanged with 10 phr of modified GTR.

The mechanical performance of filled rubber composites is highly dependent on the degree of adhesion between the filler and the rubber matrices, as well as on the cross-link density. As previously stated, the migration of sulfur from the rubber matrix to m-GTR reduces the cross-link density and would decrease the mechanical strength, correspondingly. However, the chemical nature of the filler surface also plays an important role in the reinforcing action. Changes in the chemical structure of m-GTR due to the H_2SO_4 oxidizing treatment influenced its adhesion ability with regard to the SBR matrix, and thus altered the mechanical properties of the filled SBR vulcanizates. Such improvement can be ascribed to the creation of new oxygen-containing polar functional groups, due to the improved interfacial bonding between the modified GTR and the SBR matrix [24]. Furthermore, the H_2SO_4 chemical treatment created more carbon–carbon double bonds (C=C) on the surface of the m-GTR, as displayed in the FTIR spectra (Figure 4). These unsaturated bonds can interact with the equivalent bonds existing in the butadiene part of the SBR matrix and, to a lesser extent, in the NR and SBR fractions of the GTR, leading to an improved interfacial adhesion. In this sense, there are two processes taking place simultaneously: the vulcanization of the virgin rubber (SBR) and the re-vulcanization of partially devulcanized GTR (NR and SBR fractions) during the vulcanization processes of rubber composites [41].

SEM was used to corroborate the adhesion between the GTR and the SBR matrix. Figure 8 shows the fractographs of the samples. With the increment in GTR and m-GTR content, a more heterogeneous and rougher surface can be seen and some agglomerates start to appear. The GTR and m-GTR aggregates could reaggregate with each other during the vulcanization process and limit the uniform distribution of GTR and m-GTR in the SBR matrix, regardless of the modification carried out. The quality of almost every filled composite was highly dependent on the degree of dispersion the filler achieved throughout the matrix [46].

3.2.2. Dynamic Mechanical Properties

Figure 9 shows the influence of the GTR and m-GTR content on the storage modulus (E') and loss tangent ($\tan\delta$) as a function of temperature. The lowest values of E' in the glassy region were observed for the unfilled SBR; however, GTR and m-GTR content increased this property. This increase can be ascribed to the carbon black present in the GTR (50 phr) [17], restricting the mobility of the polymer chains and providing rigidity to the vulcanized compounds. The $\tan\delta$ curves show a peak temperature (i.e., glass transition temperature- T_g) localized around $-36\text{ }^\circ\text{C}$ that did not change significantly with the type of GTR or with its content (Table 7). Moreover, the variation in the intensity of the $\tan\delta$ peak suggests that the increase in the filler content promoted the elastic behavior ($\tan\delta_{\max}$ reduction); the addition of GTR and m-GTR reduced the losses due to the internal friction of the molecular chains in the T_g region. Thus, less energy was required for the movement of the molecular chains as they approached the transition from the glassy to the rubbery state and this can be correlated with the reduced mobility of the polymer chains at the matrix-filler interface [47]. The adhesion parameter (A) can explain the interfacial interactions between SBR and the sustainable filler. A low value for A indicates a high level of interface adhesion and enhanced interactions between the matrix and filler particles (Table 7). The SBR-10-mGTR composite had the lowest values for the adhesion parameter (0.2503), which corroborated with better adhesion at the matrix-m-GTR interface [39].

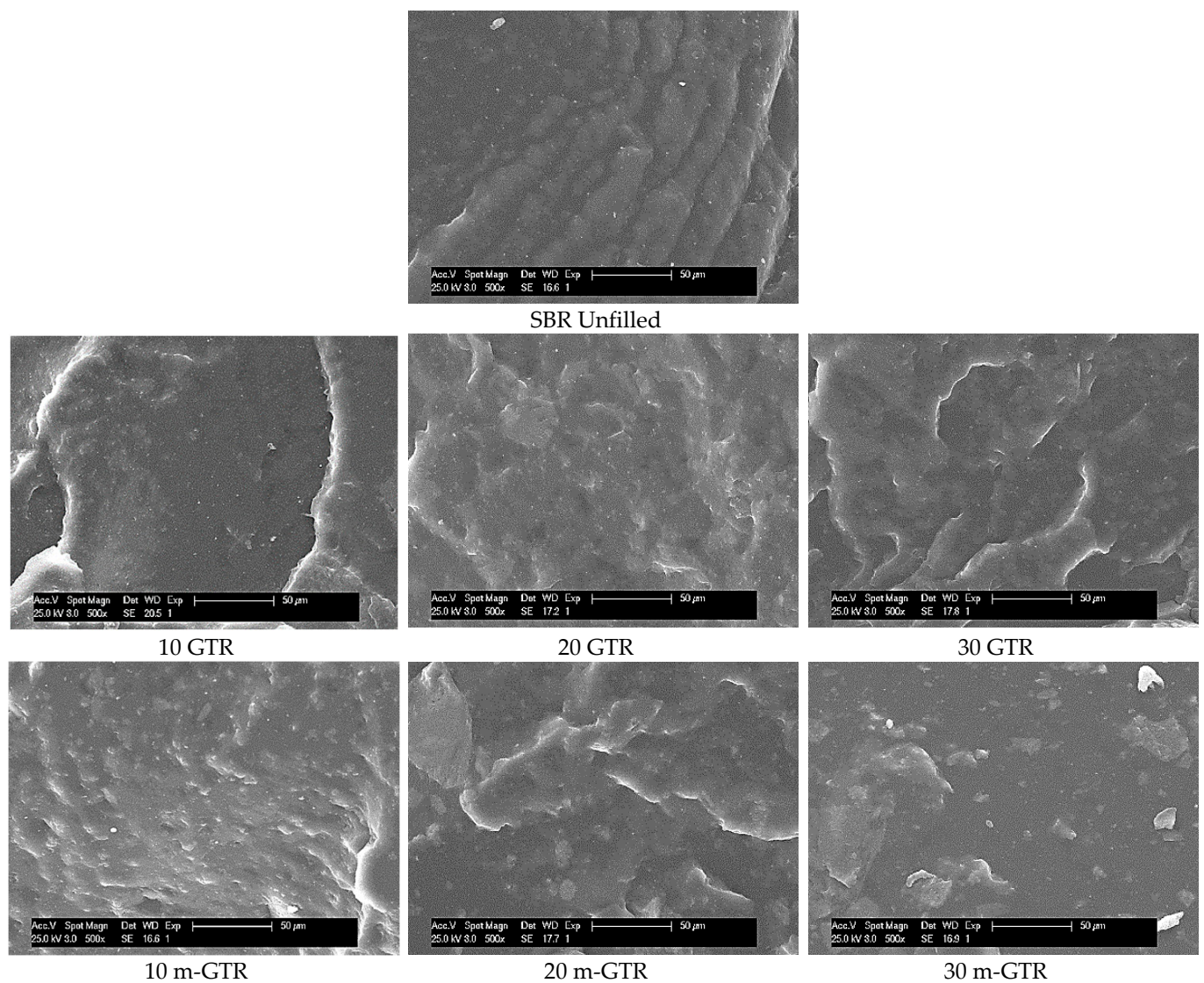


Figure 8. SEM fractographs of the unfilled and filled composites with different GTR and m-GTR content.

Table 7. Dynamic-mechanical properties of GTR-SBR and m-GTR-SBR composites.

Composite	Unfilled (SBR)	10 GTR	20 GTR	30 GTR	10 m-GTR	20 m-GTR	30 m-GTR
T_g ($\tan\delta$ max) ($^{\circ}\text{C}$)	−35.4	−35.8	−36.7	−36.9	−35.5	−36.3	−36.6
$\tan\delta$ at 25 $^{\circ}\text{C}$	0.1404	0.1653	0.1750	0.1871	0.1628	0.1941	0.2103
E' at 25 $^{\circ}\text{C}$ (MPa)	2.68	3.16	3.59	3.91	3.22	3.98	4.73
Adhesion factor, A	-	0.2696	0.4421	0.6582	0.2503	0.5948	0.8498
$\tan\delta$ at −10 $^{\circ}\text{C}$	0.1663	0.1741	0.1676	0.1829	0.1665	0.1398	0.1428
$\tan\delta$ at 60 $^{\circ}\text{C}$	0.1241	0.1710	0.1950	0.2195	0.1721	0.2416	0.2742

The $\tan\delta$ is of great value for the tire industry, since it is frequently used to predict the wet grip and the rolling resistance of tire treads. These two material-specific requirements, together with the abrasion resistance, form the so-called “magic triangle” of tires: searching for driving safety, lower fuel consumption and extended lifetime, respectively.

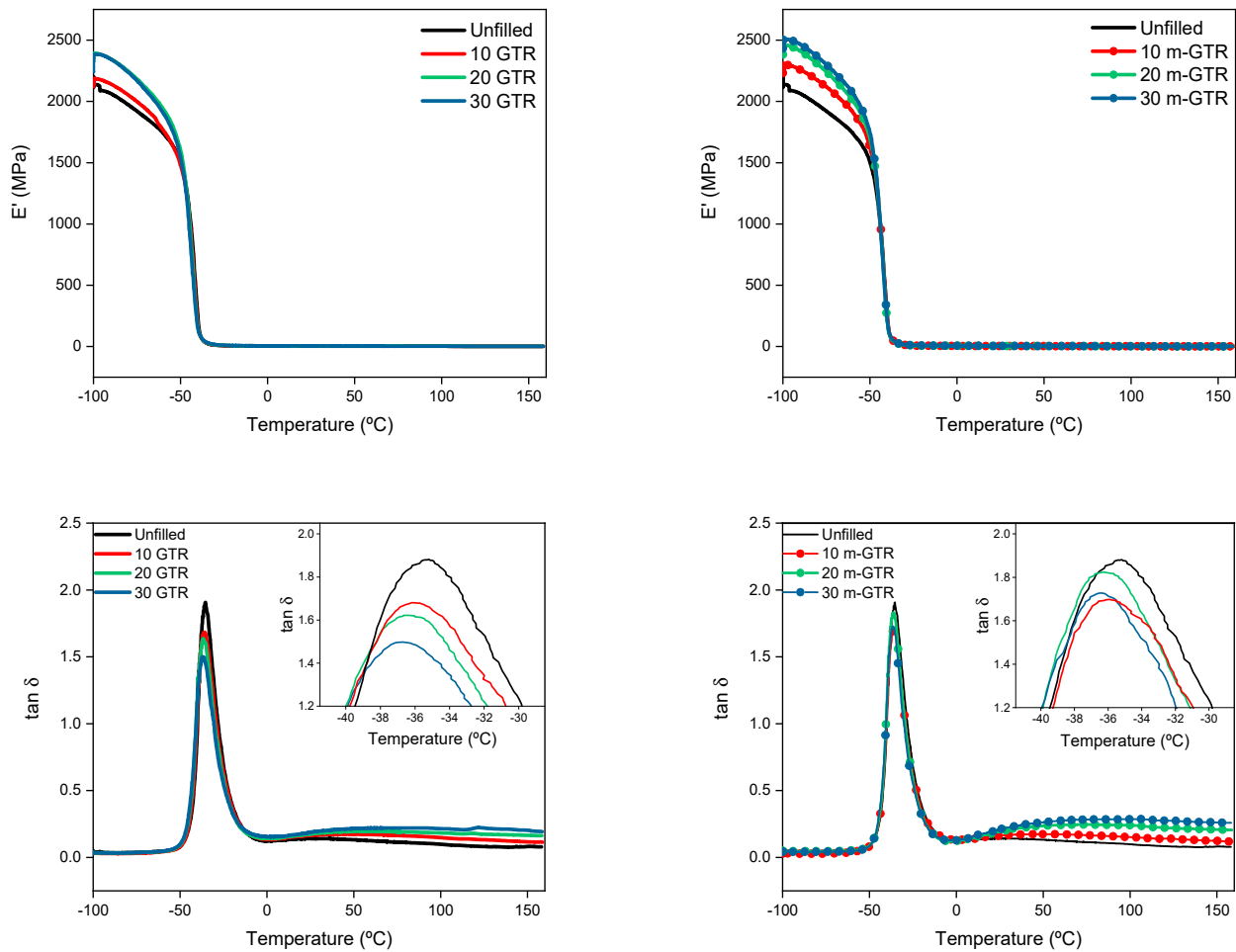


Figure 9. Storage modulus (E') and loss tangent ($\tan\delta$) of SBR-GTR and SBR-m-GTR composites.

At low temperatures (-10 – 0 °C), the value of $\tan\delta$ corresponds to the wet grip efficiency, a very important characteristic in the safety of a tire. A high value of $\tan\delta$ at this temperature is necessary to achieve greater resistance to wet skidding. On the other hand, at high temperatures (60 °C), similar to those reached by the tire in motion, the value of $\tan\delta$ is related to the rolling resistance of the tire, where a low value of $\tan\delta$ is necessary to achieve a low rolling resistance in order to save energy. Hence, the ideal condition achievable, a low $\tan\delta$ at 60 °C and a high $\tan\delta$ at -10 °C, would guarantee lower rolling resistance and better fuel economy and assure appropriate wet traction simultaneously. Table 7 shows $\tan\delta$ values in the two mentioned temperature ranges. The inclusion of GTR and m-GTR did not result in an improved rolling resistance. Nonetheless, a positive effect was observed for the wet grip, for which the inclusion of the filler maintained, and even slightly increased, $\tan\delta$ values. Future work will deal with the study of all three requirements of the magic triangle, as well as with the improvement of mechanical strength in order to achieve suitability for tire applications.

4. Conclusions

The aim of the present work was to study SBR composites filled with mechano-chemically modified GTR in order to overcome the poor compatibility between the waste material and the rubber matrix. The mechano-chemical modification of GTR was realized following two steps: (i) a cryo-grinding process; (ii) different oxidizing treatments. The cryo-grinding process was successfully optimized, reducing the average particle size of the departing material to 100 – 150 μm , achieving a narrow distribution and a smooth fracture surface. The oxidation on the surface of GTR was corroborated by the increase in oxygen

content, the modification with H₂SO₄ being the most successful one. The interaction of the polar functional groups in the surface of GTR with the SBR matrix favored the adhesion between phases and improved the mechanical performance of the composite, achieving an increase of 115% in tensile strength and 712% in elongation at break, with only 10 phr of the modified GTR. These results serve as a departing point for the development of sustainable rubber composites, recycling a waste material as reinforcing filler and contributing to the circular economy model.

Supplementary Materials: The following are available online at <https://www.mdpi.com/2504-477X/5/3/68/s1>, Figure S1: Particle size distribution of cryo-ground GTR and chemically modified GTR (m-GTR). Figure S2: C and O core spectra of: (a) and (b) GTR; (c) and (d) GTR Cryo; (e) and (f) GTR modified with H₂O₂; (g) and (h) GTR modified with H₂SO₄; (i) and (j) GTR modified with HNO₃; (k) and (l) GTR modified with H₂SO₄/HNO₃. Table S1: Average particle size and diameter on cumulative percentage for cryo-ground GTR (GTR Cryo) and chemically modified GTR (m-GTR).

Author Contributions: J.A.-M.: Conceptualization, Methodology, Validation, Investigation, Data curation, Formal analysis, Writing—original draft, Writing—review and editing, Visualization; R.V.-M.: Methodology; S.G.: Methodology; R.V.: Conceptualization, Validation, Writing—review and editing, Visualization, Project administration, Funding acquisition; M.A.L.-M.: Conceptualization, Validation, Writing—review and editing, Visualization; M.H.S.: Conceptualization, Methodology, Validation, Resources, Data curation, Writing—original draft, Writing—review and editing, Visualization, Supervision, Project administration, Funding acquisition. All authors have read and agreed to the published version of the manuscript.

Funding: This research was funded by the State Research Agency of Spain (AEI) through grants PID2019-107501RB-I00 and RYC2017-22837, and by the Community of Madrid through a research assistant contract (PEJ 2019-AI/IND-1635).

Acknowledgments: All the authors acknowledge Arlanxeo and Signus Ecovalor for kindly providing the SBR and GTR, respectively.

Conflicts of Interest: The authors declare no conflict of interest.

References

1. Ellen MacArthur Foundation. Available online: <https://www.ellenmacarthurfoundation.org/explore/the-circular-economy-in-detail> (accessed on 27 October 2020).
2. Zefeng, W.; Yong, K.; Zhao, W.; Yi, C. Recycling waste tire rubber by water jet pulverization: Powder characteristics and reinforcing performance in natural rubber composites. *J. Polym. Eng.* **2018**, *38*, 51–62. [[CrossRef](#)]
3. Hoyer, S.; Kroll, L.; Sykutera, D. Technology comparison for the production of fine rubber powder from end of life tyres. *Procedia Manuf.* **2020**, *43*, 193–200. [[CrossRef](#)]
4. Petrella, A.; Notarnicola, M. Lightweight Cement Conglomerates Based on End-of-Life Tire Rubber: Effect of the Grain Size, Dosage and Addition of Perlite on the Physical and Mechanical Properties. *Materials* **2021**, *14*, 225. [[CrossRef](#)] [[PubMed](#)]
5. Liang, M.; Sun, C.; Yao, Z.; Jiang, H.; Zhang, J.; Ren, S. Utilization of wax residue as compatibilizer for asphalt with ground tire rubber/recycled polyethylene blends. *Constr. Build. Mater.* **2020**, *230*, 116966. [[CrossRef](#)]
6. Ameli, A.; Maher, J.; Mosavi, A.; Nabipour, N.; Babagoli, R.; Norouzi, N. Performance evaluation of binders and Stone Matrix Asphalt (SMA) mixtures modified by Ground Tire Rubber (GTR), waste Polyethylene Terephthalate (PET) and Anti Stripping Agents (ASAs). *Constr. Build. Mater.* **2020**, *251*, 118932. [[CrossRef](#)]
7. Yagneswaran, S.; Storer, W.J.; Tomar, N.; Chaur, M.N.; Echegoyen, L.; Smith, D.W. Surface-grafting of ground rubber tire by poly acrylic acid via self-initiated free radical polymerization and composites with epoxy thereof. *Polym. Compos.* **2013**, *34*, 769–777. [[CrossRef](#)]
8. Formela, K.; Hejna, A.; Zedler, Ł.; Przybysz, M.; Ryl, J.; Saeb, M.R.; Piszczyk, Ł. Structural, thermal and physico-mechanical properties of polyurethane/brewers' spent grain composite foams modified with ground tire rubber. *Ind. Crop. Prod.* **2017**, *108*, 844–852. [[CrossRef](#)]
9. Aoudia, K.; Azem, S.; Hocine, N.A.; Gratton, M.; Pettarin, V.; Seghar, S. Recycling of waste tire rubber: Microwave devulcanization and incorporation in a thermoset resin. *Waste Manag.* **2017**, *60*, 471–481. [[CrossRef](#)]
10. Hejna, A.; Korol, J.; Przybysz-Romatowska, M.; Zedler, Ł.; Chmielnicki, B.; Formela, K. Waste tire rubber as low-cost and environmentally-friendly modifier in thermoset polymers—A review. *Waste Manag.* **2020**, *108*, 106–118. [[CrossRef](#)] [[PubMed](#)]
11. de Sousa, F.D.B.; Gouveia, J.R.; De Camargo Filho, P.M.F.; Vidotti, S.E.; Scuracchio, C.H.; Amurin, L.G.; Valera, T.S. Blends of ground tire rubber devulcanized by microwaves/HDPE—Part A: Influence of devulcanization process. *Polimeros* **2015**, *25*, 256–264. [[CrossRef](#)]

12. de Sousa, F.D.B.; Gouveia, J.R.; De Camargo Filho, P.M.F.; Vidotti, S.E.; Scuracchio, C.H.; Amurin, L.G.; Valera, T.S. Blends of ground tire rubber devulcanized by microwaves/HDPE-Part B: Influence of clay addition. *Polimeros* **2015**, *25*, 382–391. [[CrossRef](#)]
13. Rosas, R.M.M.; Genescá, M.M.; Ballart-Prunell, J. Dielectric properties of various polymers (PVC, EVA, HDPE, and PP) reinforced with ground tire rubber (GTR). *Sci. Eng. Compos. Mater.* **2015**, *22*, 231–243. [[CrossRef](#)]
14. Yehia, A.A.; Ismail, M.N.; Hefny, Y.A.; Abdel-Bary, E.M.; Mull, M.A. Mechano-chemical reclamation of waste rubber powder and its effect on the performance of NR and SBR vulcanizates. *J. Elastomers Plast.* **2004**, *36*, 109–123. [[CrossRef](#)]
15. Carli, L.N.; Bianchi, O.; Mauler, R.S.; Crespo, J.S. Crosslinking kinetics of SBR composites containing vulcanized ground scraps as filler. *Polym. Bull.* **2011**, *67*, 1621–1631. [[CrossRef](#)]
16. Formela, K.; Formela, M.; Thomas, S.; Haponiuk, J. Styrene-Butadiene Rubber/Modified Ground Tire Rubber Blends Co-Vulcanization: Effect of Accelerator Type. *Macromol. Symp.* **2016**, *361*, 64–72. [[CrossRef](#)]
17. Santana, M.H.; Huete, M.; Lameda, P.; Araujo, J.; Verdejo, R.; López-Manchado, M.A. Design of a new generation of sustainable SBR compounds with good trade-off between mechanical properties and self-healing ability. *Eur. Polym. J.* **2018**, *106*, 273–283. [[CrossRef](#)]
18. Araujo-Morera, J.; Santana, M.H.; Verdejo, R.; López-Manchado, M.A. Giving a Second Opportunity to Tire Waste: An Alternative Path for the Development of Sustainable Self-Healing Styrene-Butadiene Rubber Compounds Overcoming the Magic Triangle of Tires. *Polymers* **2019**, *11*, 2122. [[CrossRef](#)]
19. Zedler, Ł.; Colom, X.; Cañavate, J.; Saeb, M.R.; Haponiuk, J.T.; Formela, K. Investigating the Impact of Curing System on Structure-Property Relationship of Natural Rubber Modified with Brewery By-Product and Ground Tire Rubber. *Polymers* **2020**, *12*, 545. [[CrossRef](#)]
20. Fazli, A.; Rodrigue, D. Recycling Waste Tires into Ground Tire Rubber (GTR)/Rubber Compounds: A Review. *J. Compos. Sci.* **2020**, *4*, 103. [[CrossRef](#)]
21. Majewska-Laks, K.; Sykutera, D.; Ościak, A. Reuse of ground tire rubber (GTR) as a filler of TPE matrix*. *MATEC Web Conf.* **2021**, *332*, 01003. [[CrossRef](#)]
22. Zedler, Ł.; Przybysz-Romatowska, M.; Haponiuk, J.; Wang, S.; Formela, K. Modification of Ground Tire Rubber—Promising Approach for Development of Green Composites. *J. Compos. Sci.* **2019**, *4*, 2. [[CrossRef](#)]
23. Maridass, B.; Gupta, B.R. Effect of Carbon Black on Devulcanized Ground Rubber Tire—Natural Rubber Vulcanizates: Cure Characteristics and Mechanical Properties. *J. Elastomers Plast.* **2006**, *38*, 211–229. [[CrossRef](#)]
24. Cheng, X.; Long, D.; Huang, S.; Li, Z.; Guo, X. Time effectiveness of the low-temperature plasma surface modification of ground tire rubber powder. *J. Adhes. Sci. Technol.* **2015**, *29*, 1330–1340. [[CrossRef](#)]
25. Li, J.; Yao, S.; Xiao, F.; Amirkhanian, S.N. Surface modification of ground tire rubber particles by cold plasma to improve compatibility in rubberised asphalt. *Int. J. Pavement Eng.* **2020**, *1*–12. [[CrossRef](#)]
26. Cataldo, F.; Ursini, O.; Angelini, G. Surface oxidation of rubber crumb with ozone. *Polym. Degrad. Stab.* **2010**, *95*, 803–810. [[CrossRef](#)]
27. Cao, X.-W.; Luo, J.; Cao, Y.; Yin, X.-C.; He, G.-J.; Peng, X.-F.; Xu, B.-P. Structure and properties of deeply oxidized waster rubber crumb through long time ozonization. *Polym. Degrad. Stab.* **2014**, *109*, 1–6. [[CrossRef](#)]
28. Herrera-Sosa, E.S.; Martínez-Barrera, G.; Barrera-Díaz, C.E.; Cruz-Zaragoza, E.; Martí Nez-Barrera, G.; Dí, B.; Az, C. Waste Tire Particles and Gamma Radiation as Modifiers of the Mechanical Properties of Concrete. *Adv. Mater. Sci. Eng.* **2014**, *2014*, 1–7. [[CrossRef](#)]
29. Shanmugaraj, A.; Kim, J.K.; Ryu, S.H. UV surface modification of waste tire powder: Characterization and its influence on the properties of polypropylene/waste powder composites. *Polym. Test.* **2005**, *24*, 739–745. [[CrossRef](#)]
30. Yehia, A.A.; Mull, M.A.; Ismail, M.N.; Hefny, Y.A.; Abdel-Bary, E.M. Effect of chemically modified waste rubber powder as a filler in natural rubber vulcanizates. *J. Appl. Polym. Sci.* **2004**, *93*, 30–36. [[CrossRef](#)]
31. Colom, X.; Carrillo, F.; Cañavate, J. Composites reinforced with reused tyres: Surface oxidant treatment to improve the interfacial compatibility. *Compos. Part A Appl. Sci. Manuf.* **2007**, *38*, 44–50. [[CrossRef](#)]
32. Colom, X.; Cañavate, J.; Carrillo, F.; Suñol, J.J. Effect of the particle size and acid pretreatments on compatibility and properties of recycled HDPE plastic bottles filled with ground tyre powder. *J. Appl. Polym. Sci.* **2009**, *112*, 1882–1890. [[CrossRef](#)]
33. Gámez, J.F.H.; Hernández, E.H.; Céspedes, R.I.N.; Velázquez, M.G.N.; Rosales, S.G.S.; Corral, F.S.; Morones, P.G.; Tavizón, S.F.; De León, R.D.; Cepeda, L.F. Mechanical reinforcement of thermoplastic vulcanizates using ground tyre rubber modified with sulfuric acid. *Polym. Compos.* **2016**, *39*, 229–237. [[CrossRef](#)]
34. Hernández, E.H.; Gámez, J.F.H.; Cepeda, L.F.; Muñoz, E.J.C.; Corral, F.S.; Rosales, S.G.S.; Velázquez, G.N.; Morones, P.G.; Martínez, D.I.S. Sulfuric acid treatment of ground tire rubber and its effect on the mechanical and thermal properties of polypropylene composites. *J. Appl. Polym. Sci.* **2017**, *134*, 1–7. [[CrossRef](#)]
35. Naskar, A.K.; De, S.K.; Bhowmick, A.K. Thermoplastic elastomeric composition based on maleic anhydride-grafted ground rubber tire. *J. Appl. Polym. Sci.* **2002**, *84*, 370–378. [[CrossRef](#)]
36. Aggour, Y.A.; Al-Shihri, A.S.; Bazzt, M.R. Surface Modification of Waste Tire by Grafting with Styrene and Maleic Anhydride. *Open J. Polym. Chem.* **2012**, *2*, 70–76. [[CrossRef](#)]
37. Rungrodnimitchai, S.; Kotatha, D. Chemically modified ground tire rubber as fluoride ions adsorbents. *Chem. Eng. J.* **2015**, *282*, 161–169. [[CrossRef](#)]

38. Flory, P.J.; Rehner, J., Jr. Statistical mechanics of cross-linked polymer networks II. Swelling. *J. Chem. Phys.* **1943**, *11*, 521–526. [[CrossRef](#)]
39. Midhun Dominic, C.D.; Joseph, R.; Begum, P.M.S.; Joseph, M.; Padmanabhan, D.; Morris, L.A.; Kumar, A.S.; Formela, K. Cellulose nanofibers isolated from the cuscuta reflexa plant as a green reinforcement of natural rubber. *Polymers* **2020**, *12*, 814. [[CrossRef](#)]
40. Liang, H.; Gagné, J.D.; Faye, A.; Rodrigue, D.; Brisson, J. Ground tire rubber (GTR) surface modification using thiol-ene click reaction: Polystyrene grafting to modify a GTR/polystyrene (PS) blend. *Prog. Rubber Plast. Recycl. Technol.* **2019**, *36*, 81–101. [[CrossRef](#)]
41. Xinxing, Z.; Xiaoqing, Z.; Mei, L.; Canhui, L. Improvement of the properties of ground tire rubber (GTR)-filled nitrile rubber vulcanizates through plasma surface modification of GTR powder. *J. Appl. Polym. Sci.* **2009**, *114*, 1118–1125.
42. Gibala, D.; Thomas, D.; Hamed, G.R. Cure and Mechanical Behavior of Rubber Compounds Containing Ground Vulcanizates: Part III. Tensile and Tear Strength. *Rubber Chem. Technol.* **1999**, *72*, 357–360. [[CrossRef](#)]
43. Choi, S.-S.; Park, B.-H.; Song, H. Influence of filler type and content on properties of styrene-butadiene rubber(SBR) compound reinforced with carbon black or silica. *Polym. Adv. Technol.* **2004**, *15*, 122–127. [[CrossRef](#)]
44. Nelson, P.; Kutty, S. Cure Characteristics and Mechanical Properties of Butadiene Rubber/Whole Tyre Reclaimed Rubber Blends. *Prog. Rubber, Plast. Recycl. Technol.* **2002**, *18*, 85–97. [[CrossRef](#)]
45. Kang, M.-J.; Heo, Y.-J.; Jin, F.-L.; Park, S.-J. A review: Role of interfacial adhesion between carbon blacks and elastomeric materials. *Carbon Lett.* **2016**, *18*, 1–10. [[CrossRef](#)]
46. Dai, S.-Y.; Ao, G.-Y.; Kim, M.-S. Properties of Carbon Black/SBR Rubber Composites Filled by Surface Modified Carbon Blacks. *Carbon Lett.* **2007**, *8*, 115–119. [[CrossRef](#)]
47. Formela, K.; Hejna, A.; Piszczyk, Ł.; Saeb, M.R.; Colom, X. Processing and structure–property relationships of natural rubber/wheat bran biocomposites. *Cellulose* **2016**, *23*, 3157–3175. [[CrossRef](#)]